Indian Journal of Pure & Applied Physics
Vol. 63, November 2025, pp. 1014-1022
DOI: 10.56042/ijpap.v63i11.21770

# Ultrafast All Optical N-Bit Comparator Using 2D Photonic Crystals with Hexagonal Lattice Structure

Kajal Maji[a] & Kousik Mukherjee[a,b*]

[a]Department of Physics, Banwarilal Bhalotia College, Asansol 713 303, India

[b]Centre of Organic Spintronics and Optoelectronic devices, Kazi Nazrul University, Asansol 713 340, India

*Received:18th July 2025; accepted:29th September 2025*

The manuscript represents a design of all optical N-bit comparator using 2D photonic crystals. The device can compare two N-bit numbers by comparing the most significant bit (MSB) and successive bits serially. The device is numerically simulated for optimized performance and an operating speed of 5 Tb/s is calculated from response time diagram. The design ensures high contrast ratios, compact footprint, and scalability to higher bit levels. Numerical simulations using the finite-difference time-domain (FDTD) method confirm the efficient performance of the comparator, with an operational speed in the tera bite regime and negligible signal degradation. The proposed N-bit comparator is a promising candidate for integration in all-optical signal processing and high-speed photonic computing systems.

**Keywords:** Photonic crystal, All optical, Comparator, Serial comparison, Ultrafast operation

All optical signal processing (AOSP) needs ultra-high speed devices for practical implementation with efficient photonic integration capability. Photonic crystal (PhC) based logic gates and processors established themselves as promising candidates of future photonic network and communication systems[1] for AOSP. Photonic crystals are a new kind of structure that has periodic variations in refractive index and have unique controllable properties by varying refractive index, lattice dimensions, creating defects etc. The periodic crystal-like structure gives rise to a photonic bandgap (PBG), and certain wavelengths are forbidden to be propagated through the PhC and certain wavelengths propagate (pass bands). This happens due to constructive and destructive interference of incidents and scattered lights inside the photonic crystals. The wavelengths in the pass band propagate with a minimum attenuation. Two-dimensional (2D) photonic crystals offer compactness, high integration density, and strong light confinement capabilities, making them ideal for onchip optical computing elements. While square and triangular lattice structures have been widely investigated, the hexagonal lattice structure offers unique advantages in terms of symmetry, isotropic bandgap properties, and enhanced design flexibility for compact device implementation.

Photonic Crystals find applications in gas sensors[2], filters[3,4], neural network modelling[5], bio sensors[6] etc., beside logic gates[7-11]AND, OR, NAND, NOR, XOR, XNOR etc., and optical logic processors[12-18] like half adder(HA) and full adder (FA),comparators[14, 15]etc. Sequential circuits like flip flops are proposed using photonic crystals[16,19]. Optical logic gates, combinational and sequential logic processors are the basic building blocks for AOSP systems. Digital comparators also find applications in various AOSP like digital data processing, memory devices and arithmetic units. Therefore, different types of comparators using photonic crystals are also available by different researchers[14,15,20-26]. However, the comparators proposed so far are mainly single bit and no N bit comparator has been found using photonic crystals. Few all-optical N bit comparators using semiconductor optical amplifiers (SOA) are available, but they are complex in design and slow[27-29] due to slow carrier dynamics of the SOA. SOA based designs are complex in hardware as large numbers of SOAs are used, and since nonlinear processes are responsible for their workings, they have slow response. In contrast the present photonic crystal based devices use no nonlinearity, and therefore,

*Corresponding author: E-mail:klmukherjee003@gmail.com

operate faster than SOA based devices. The N bit comparators proposed in[27-29] used many active devices (SOAs, Add drop Multiplexers etc.), and other passive devices. This also slows down performance. Therefore, all optical comparators using photonic crystals is essential for fast AOSP systems. Moreover, most of the proposed comparators so far proposed uses some kind of nonlinearities (Kerr effect) also makes them slower. Therefore, the present communication proposes an N bit comparator using photonic crystals without using any nonlinearity with low footprint. The novelty of the proposed design is used hexagonal lattice geometry, which enhances the control over light propagation paths and improves coupling efficiency between photonic components. Simulation results using the finite-difference time-domain (FDTD) method demonstrate the functional correctness of the comparator, as well as its potential for high-speed, low-power, and highly integrated photonic computing applications.

## 2 Method

### 2.1 Working of all Optical N Bit Comparator:

The block diagram of N bit comparator is shown in the Fig.1 below. The basic unit has two inputs $A_j$ and $B_j$, and outputs $X_j$, $Y_j$ and $Z_j$. The algorithm of the proposed comparison method is as follows[29]: Table 1 shows the basic operations of the proposed N bit comparator. Two numbers A = $A_nA_{n-1}A_{n-2}$…..$A_1A_0$ and B = $B_nB_{n-1}B_{n-2}$…..$B_1B_0$enter serially and simultaneously starting from most significant bits(MSBs) first and then successively up to least significant bits(LSBs). When the respective bits of these two numbers A and B enter the device, four different situations may arise as shown in Table 1. Suppose the significant bits of the two numbers are equal i.e., both are 1(or 0), i.e., $A_j$= $A_n$ = 1(0), and $B_j$ = $B_n$ = 1(or 0), from the design of the comparator it is found that $Y_j$ = $A_j$ X-OR $B_j$ = 0, $X_j$ = 0, and $Y_j$ = 0. These three zeros in three outputs ensure equality of the input bits. Therefore, the next bits should be compared. If the next bits are also equal, again all these three outputs will be zero. If there is a mismatch between two corresponding bits of two numbers A and B, i.e., in case of inequality between A and B, the output $Y_j$ will be 1. This output '1' in $Y_j$ ensures inequality of the two numbers. Table 2 shows that when bits are unequal $Y_j$ is always '1'. Now to check which number A or B is greater we must see the outputs $X_j$ and $Y_j$ also. In the case of $A_j$ = 0, and $B_j$ = 1, i.e., in case of A< B, $X_j$ will be '1', and $Y_j$ will be '0'. Therefore, by observing these combinations of outputs it can be infer that A is less than B, and there is no need to compare the numbers further. Similarly for the case A > B, $Y_j$ will become '1' and $X_j$ will become '0'. It is interesting to note that by observing $Y_j$ only one can decide to stop the process of comparison of two N bit numbers. This also speeds up the process of comparison and requires less circuit complexity.

### 2.2 Theoretical Modelling:

Theoretical modelling of the photonic crystals is well addressed in different literatures [10,11,14,15,17, 30-32]. The Physics of the flow of light is governed by the Maxwells equations:

$$\vec{\nabla} \times \vec{H} - \sigma\vec{E} = \partial\vec{D}/\partial t \quad \ldots (1)$$

$$-\vec{\nabla} \times \vec{E} - \sigma^*\vec{H} = \frac{\partial\vec{B}}{\partial t} \quad \ldots (2)$$

$$\vec{\nabla} \cdot \vec{D} = 0 \quad \ldots (3)$$

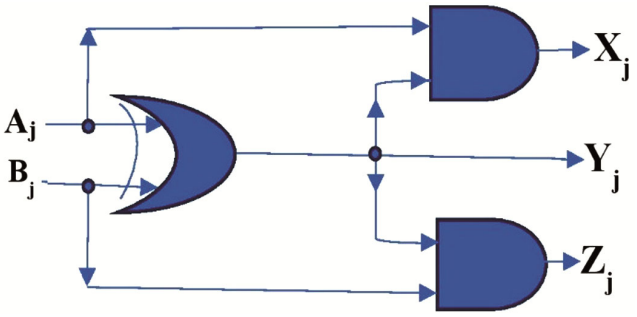


Fig. 1 — Block diagram of N-Bit Comparator

Table 1 — Truth table of N-bit Comparator

| Input | | Output | | |
|---|---|---|---|---|
| $A_j$ | $B_j$ | $X_j$ | $Y_j$ | $Z_j$ |
| 0 | 0 | 0 | 0 | 0 |
| 0 | 1 | 0 | 1 | 1 |
| 1 | 0 | 1 | 1 | 0 |
| 1 | 1 | 0 | 0 | 0 |

Table 2 — Simulation parameter table

| Parameter | Value |
|---|---|
| Refractive index | 3.42 |
| Wavelength | 1.55 μm |
| Lattice parameter | 0.566 μm |
| Response time | 136 fs |
| Bit rate | 5 Tb/s |
| Rod radius | 0.1698 μm |
| Footprint area | 392.43 $\mu m^2$ |
| Lattice dimensions | 35a×35a |

$$\vec{\nabla} \cdot \vec{E} = 0 \quad \ldots (4)$$

where E, H, D and B are electric, magnetic field vectors, σ, σ* are the electric conductivity and magnetic loss. In a linear, isotopic, non-dispersive materials D and B are related to E and H

$$\vec{D} = \varepsilon\vec{E}, and\ \vec{B} = \mu\vec{H} \quad \ldots (5)$$

where μ and ε are the permittivity and permeability. Using the Eq. (5), obtain

$$\frac{\partial\vec{H}}{\partial t} = -\frac{1}{\mu}\nabla \times \vec{E} - \frac{1}{\mu}\sigma^*\vec{H} \quad \ldots (6)$$

$$\frac{\partial\vec{E}}{\partial t} = \frac{1}{\varepsilon}\nabla \times \vec{E} - \frac{1}{\varepsilon}\sigma\vec{E} \quad \ldots (7)$$

Expansion of the curl operator of the Eqs. (6) and (7), yield the system of six coupled scalar equations[32] under Cartesian co-ordinates:

$$\frac{\partial H_x}{\partial t} = -\frac{1}{\mu}\left(\frac{\partial E_z}{\partial y} - \frac{\partial E_y}{\partial z}\right) - \frac{\sigma^*}{\mu}H_x \quad \ldots (8)$$

$$\frac{\partial H_y}{\partial t} = -\frac{1}{\mu}\left(\frac{\partial E_x}{\partial z} - \frac{\partial E_z}{\partial x}\right) - \frac{\sigma^*}{\mu}H_y \quad \ldots (9)$$

$$\frac{\partial H_z}{\partial t} = -\frac{1}{\mu}\left(\frac{\partial E_y}{\partial x} - \frac{\partial E_x}{\partial y}\right) - \frac{\sigma^*}{\mu}H_z \quad \ldots (10)$$

$$\frac{\partial E_x}{\partial t} = \frac{1}{\varepsilon}\left(\frac{\partial H_z}{\partial y} - \frac{\partial H_y}{\partial z}\right) - \frac{\sigma}{\varepsilon}E_x \quad \ldots (11)$$

$$\frac{\partial E_y}{\partial t} = \frac{1}{\varepsilon}\left(\frac{\partial H_x}{\partial z} - \frac{\partial H_z}{\partial x}\right) - \frac{\sigma}{\varepsilon}E_y \quad \ldots (12)$$

$$\frac{\partial E_z}{\partial t} = \frac{1}{\varepsilon}\left(\frac{\partial H_y}{\partial x} - \frac{\partial H_x}{\partial y}\right) - \frac{\sigma}{\varepsilon}E_z \quad \ldots (13)$$

These six-coupled equationsform the basis of FDTD simulation for modelling electromagnetic wave interactions with arbitrary 3D object. Using Yee's spatial gridding scheme[32] for 2D photonic crystals the stability condition for selecting temporal step size $\Delta t$ is determined by

$$\frac{1}{c\Delta t} \geq \sqrt{\frac{1}{(\Delta x)^2} + \frac{1}{(\Delta y)^2}} \quad \ldots (14)$$

where c is the velocity of light, $\Delta x$ and $\Delta y$ are the spatial step sizes in x and y direction respectively.

## 3 Results and Discussions

Figure 2 shows the basic structure (Fig. 2 (a)), and designed N bitcomparator with defects (Fig. 2 (b)) of N-bit comparator using 2D photonic crystals. The structure of N-bit comparator employed with hexagonal lattice with silicon of refractive index 3.42 and lattice dimension 35a×35a (a is the lattice constant). A 2D photonic crystal with a hexagonal lattice structure consists of a periodic arrangement of dielectric materials in two dimensions, typically in the form of air holes embedded in a high-index dielectric substrate, arranged in a hexagonal lattice pattern. In this structure, each unit cell contains a single rod, and the elements are spaced evenly with a lattice constant, forming a pattern where each point has six nearest neighbors at 60° intervals. This configuration introduces a periodic variation in the refractive index, enabling the formation of photonic band gaps that can prohibit the propagation of certain wavelengths of light within the plane. The hexagonal symmetry offers high packing density and can support large and complete band gaps, especially for specific polarizations (TE or TM). Footprint of the device is calculated to be 392.43 μm$^2$. Defects' radii($R_1$, $R_2$, $R_3$,

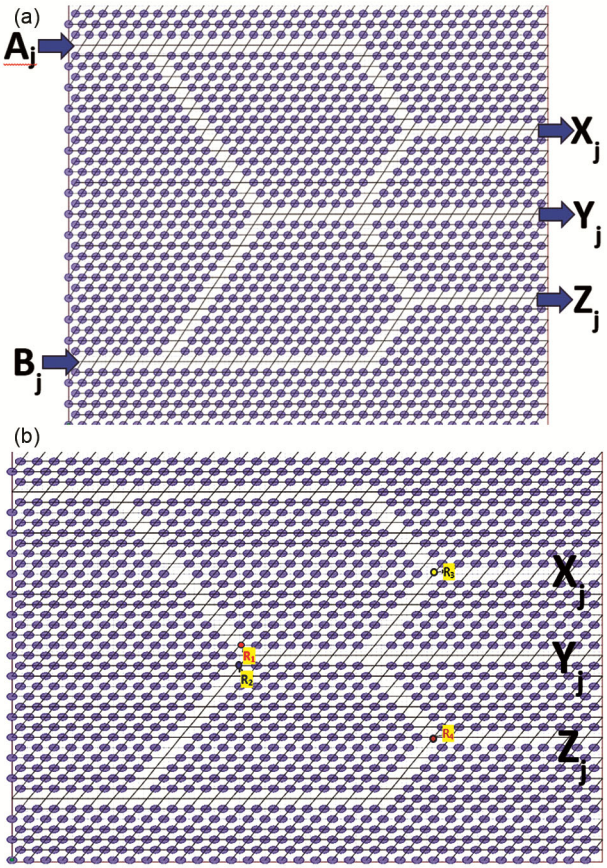


Figure 2 (a-b) –Waveguide Structure of the basic design without defects; Defects included design of the optical N-bit comparator $R_1$=$R_2$=0.1a, $R_3$=$R_4$=0.09a

and $R_4$) are to be selected for the optimized performance of the device as described below.

The photonic band structure of the device shown in the Fig. 2 is found by solving Maxwell's equations and is drawn as shown in Fig. 3 using partial wave analysis by Optiwave software.

It is interesting to note that the device shows three band gaps(PBGs) between $0.32<(w/2\pi c)<0.42$, $0.55<(w/2\pi c)<0.60$ and $0.768<(w/2\pi c)<0.833$ respectively. These PBGs correspond to the wavelength range $1341nm < \lambda < 1754nm$, $943nm < \lambda < 1029$ nm and $679nm < \lambda < 768$ nm. The wavelength range 1341 to 1754 nm includes optical window around 1.3 μm(O-BAND) corresponds to zero dispersion, around 1.55 μm(C-BAND) important because of low loss and finds applications in long haul communications. The other two bands are in the infrared (IR) and visible region. Therefore, the PBGs fall in the four important regions of wavelengths. Therefore, IR and visible light signals can also be used in this device. In the present case the rest of the simulations have been done in the wavelength region 1.51 μm to 1.61 μm which is in the C band of optical communication.

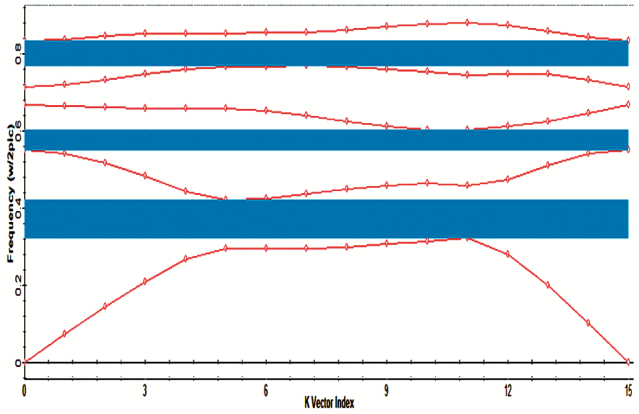


Fig. 3 — Photonic band diagram of all optical N-bit comparator

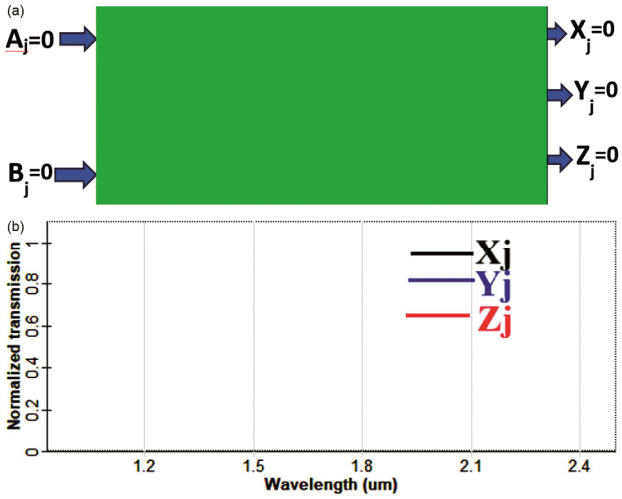


Fig. 4 — (a) Electric field distribution (b) Normalized transmission when both the inputs A=B=0 and outputs $X_i=Y_i=Z_i=0$

To investigate the performance of the N bit comparator, we have calculated extinction ratio (ER), contrast ratio (CR), and quality factor (Q)[14]. ER, CR gives the extinction between zero and 1 digital states, whereas AM represents fluctuations in the high or 1 state signals. Q signifies fluctuations in low or 0 or high or 1 state and quantify the bit error rate(BER). These quantities are optimized with respect to refractive index of the rods, radius of the rods, and wavelength used. As shown in the Table 2, the wavelength of the input signals is selected as 1.55μm, and then the refractive index and radius of the rods are varied and suitably selected (Table 2). The response time and hence operating speed of the N bit comparator are also calculated.

Figures. 4 to 7 show the electric field distribution and normalized transmission of the optical signals for different input conditions as described in table 1. In Fig. 4 and Fig. 7, all the outputs are '0's representing the equality of the $j^{th}$ bits of both the N bit numbers. Figure 5 corresponds to the case when $A_j < B_j$ and shows outputs $X_j=0$, $Y_j=1$ and $Z_j=1$, and Fig. 6 indicates $A_j > B_j$, by showing outputs $X_j=1$,

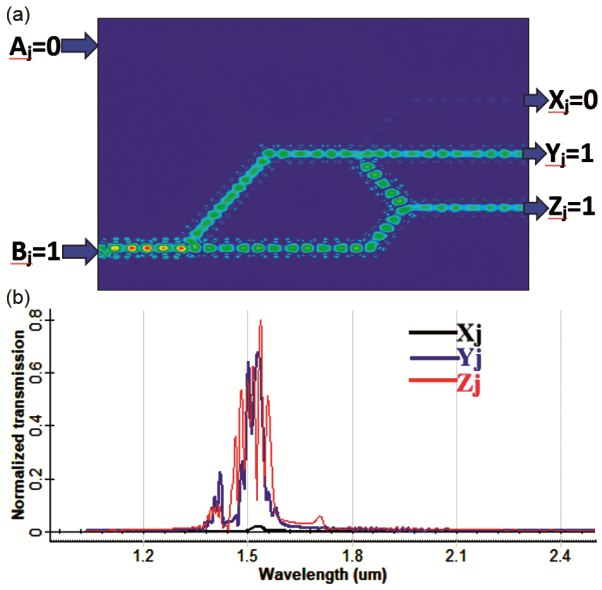


Fig. 5 — (a) Electric field distribution (b) Normalized transmission when the input A=0, Input B=1 and outputs $X_j=0$, $Y_j=1$ and $Z_j=1$

$Y_j$=1 and $Z_j$=0. The arrival of low or no signal at any of the output represents 0 bit and the presence of high intensity signals at the output represents bit 1. These low and high intensities for different low and high bit states are given in Table 3. These values of the intensities of output signal clearly indicate high extinction and contrast between 0 and 1 bits. This will be confirmed by calculating ER, CR, Q value as described in subsequent sections.

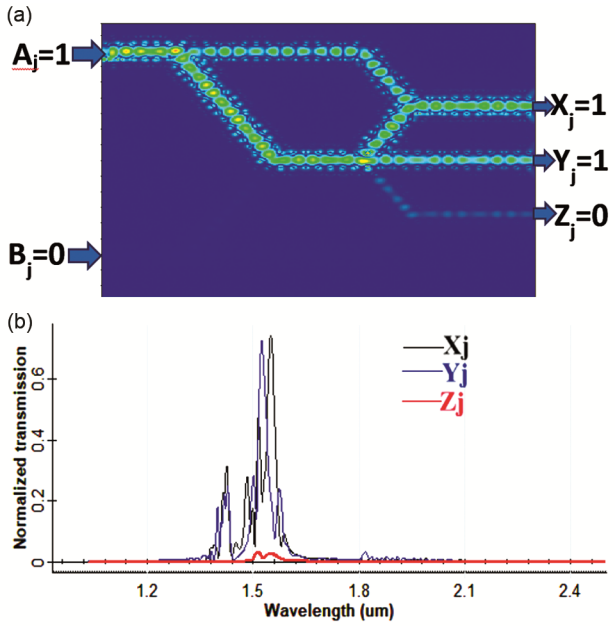


Fig. 6 — (a) Electric field distribution (b) Normalized transmission when the input A=1, Input B=0 and outputs $X_j$=1, $Y_j$=1 and $Z_j$=0

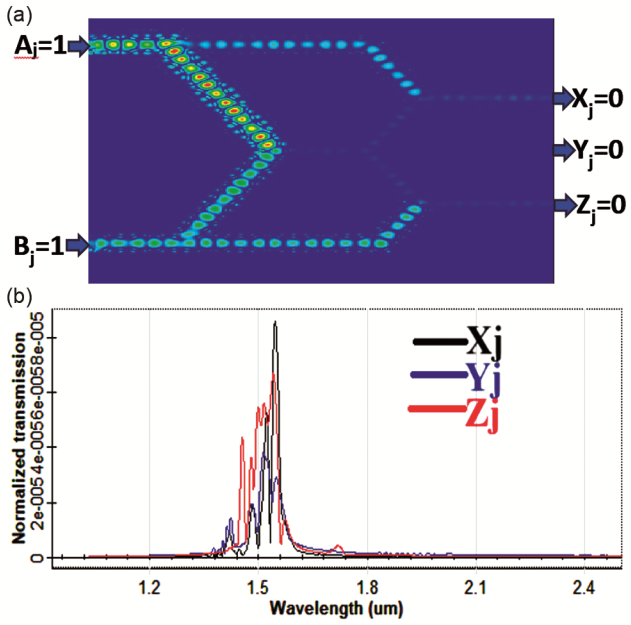


Fig. 7 — (a) Electric field distribution (b)Normalized transmission when the input A=1, Input B=1 and outputs $X_j$=0, $Y_j$=0 and $Z_j$=0

Therefore, from these Figs. 4 to 7, we may conclude that the proposed structure works as an N bit comparator. Table 3 shows corresponding normalized outputs for different input bit conditions. The table clearly indicates visible extinction between 0 and 1 states in the output signifies efficiency of the comparator.

Figure 8 shows the response time diagram of all optical N-bit comparator. From this diagram the response time of the proposed comparator is found to be 200 fs. This sharp response time corresponds to maximum operating speed of 5 Tb/s. This high speed is possibly due to the unique characteristics of photonic crystals and no use of nonlinearities like Kerr effects.

Defects into the photonic crystal structure can initiate localized modes within the photonic band gap. Resonators and waveguides are designed using these defects and can be utilized for specific applications. Moreover, by varying the size and refractive index of these defects light can be modulated inside the photonic crystals. This changes the performance of the device. Figure 9 represents the variations of (a) ER (b) CR (c) Q value of the N-bit comparator outputs Xj and Zj with refractive index and Fig. 10 shows corresponding variations for $Y_j$. All these parameters show a maximum value for refractive index 3.42.

Table 3 — Normalized output power of all optical N-bit comparators

| Input | | Normalized Output power | | |
|---|---|---|---|---|
| $A_j$ | $B_j$ | $X_j$ | $Y_j$ | $Z_j$ |
| 0 | 0 | 0 | 0 | 0 |
| 0 | 1 | 0.02 | 0.69 | 0.8 |
| 1 | 0 | 0.74 | 0.74 | 0.025 |
| 1 | 1 | 0.00008 | 0.00004 | 0.00006 |

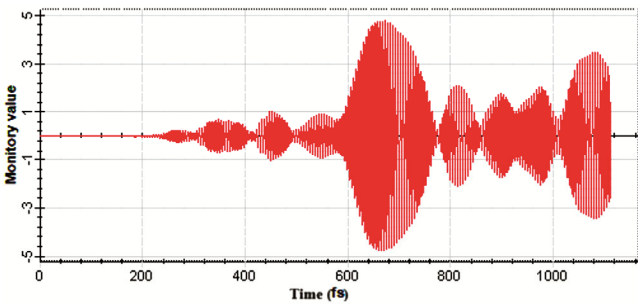


Fig. 8 — Response time diagram of all optical N-bit comparator

Radii of the defects are very important property to be investigated because these defects control the flow of the light through the photonic crystal structure by modulating scattering and interference effects. Fig. 11, and Fig. 12 show the variations of (a) ER (b) CR (c) Q value with rod radius of the N-bit comparator outputs. The optimized values of these parameters are found at rod radius 0.17μm. Finally, we investigated the dependence of these parameters (ER, CR, Q value) on the wavelength of the signals. These variations show that our selection of the wavelength at 1.55μm corresponding to minimum loss in silicon gives the optimized performance of the comparator also. Table 4 shows all these optimized parameters. The minimum ER is 15.05dB for output $Z_i$, and maximum (42.36dB) for output $Y_i$ are larger than the accepted value 10dB. The same conclusions can be drawn for the CR also. The Q value has a minimum of 28.38 also signifies a negligible BER.

After selecting the values of refractive index and rod radii, the dependence on wavelength is

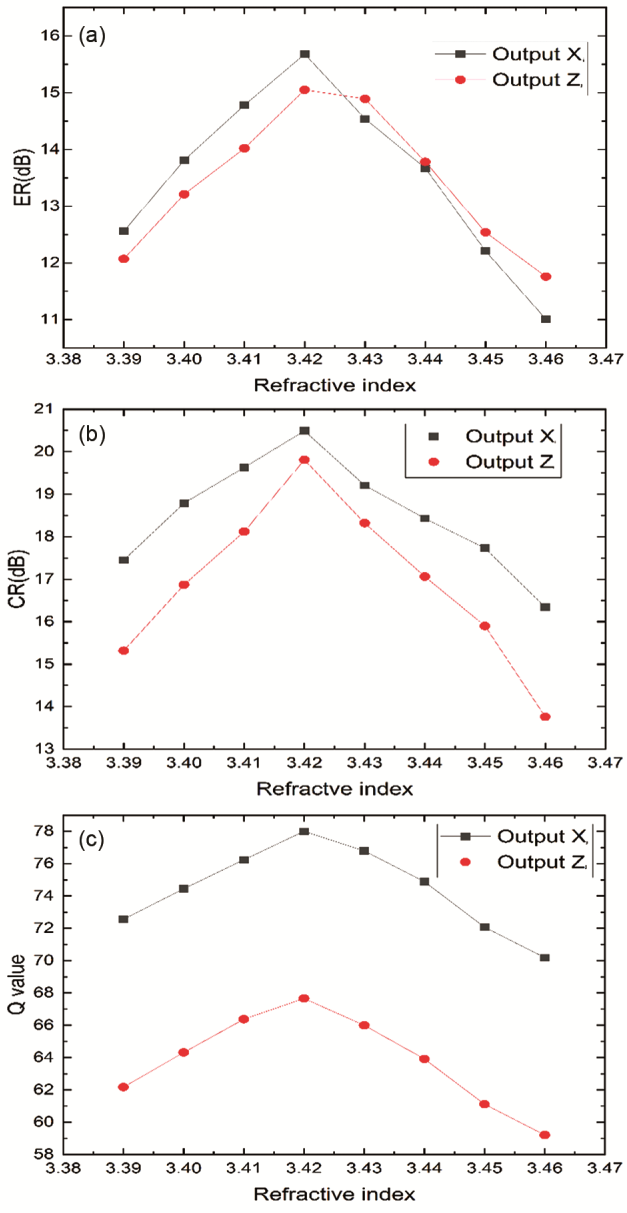


Fig. 9 — Variations of (a) ER (b) CR (c) Q value of the N-bit comparator outputs Xj and Zjwith refractive index

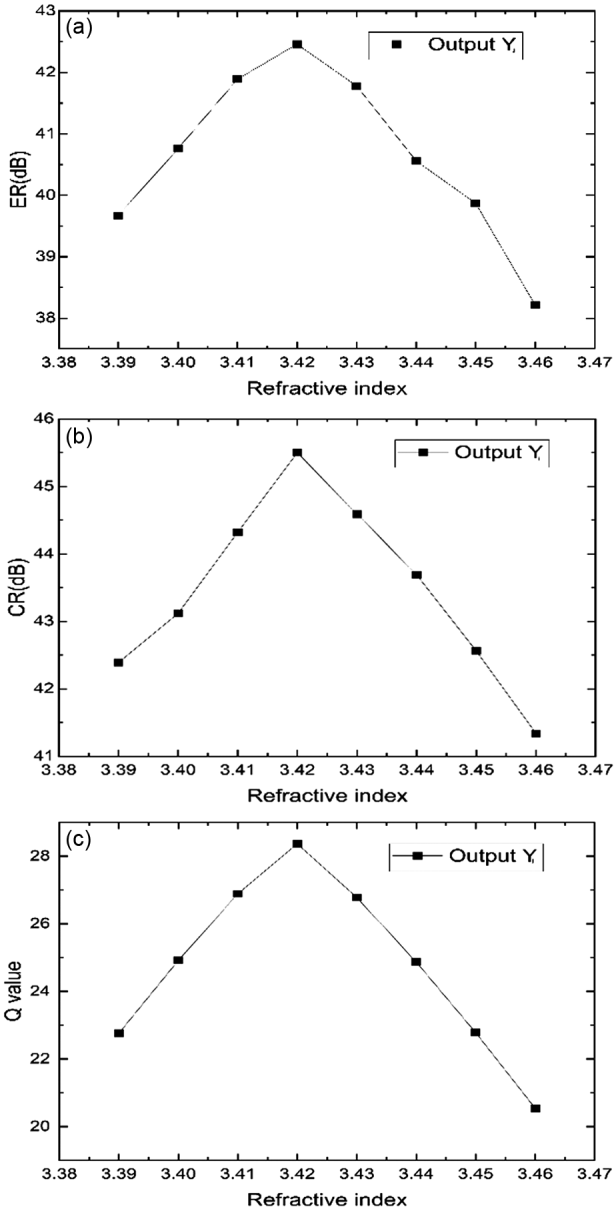


Fig. 10 — Variations of (a) ER (b) CR (c) Q value with refractive index of the N-bit comparator output Yj

considered. Figures 13 -14 show the dependence of ER, CR, and Q value with wavelength in the pass band(1.51μm to 1.61μm) of the device structure. It has been found that at wavelength 1.55μm, ER, CR, and Q values shows maximum as expected. The stability of photonic crystal-based logic devices generally ensures the reliability of the device performance in terms of maintaining the output powers in presence of internal and external variations. We have calculated the values of ER, CR, Q factor etc, and these values are optimized for different photonic crystal characteristics such as wavelength, refractive index and rod radius. The proposed design maintains distinct reliable logic states under the variations in wavelength, refractive index and rod radius.

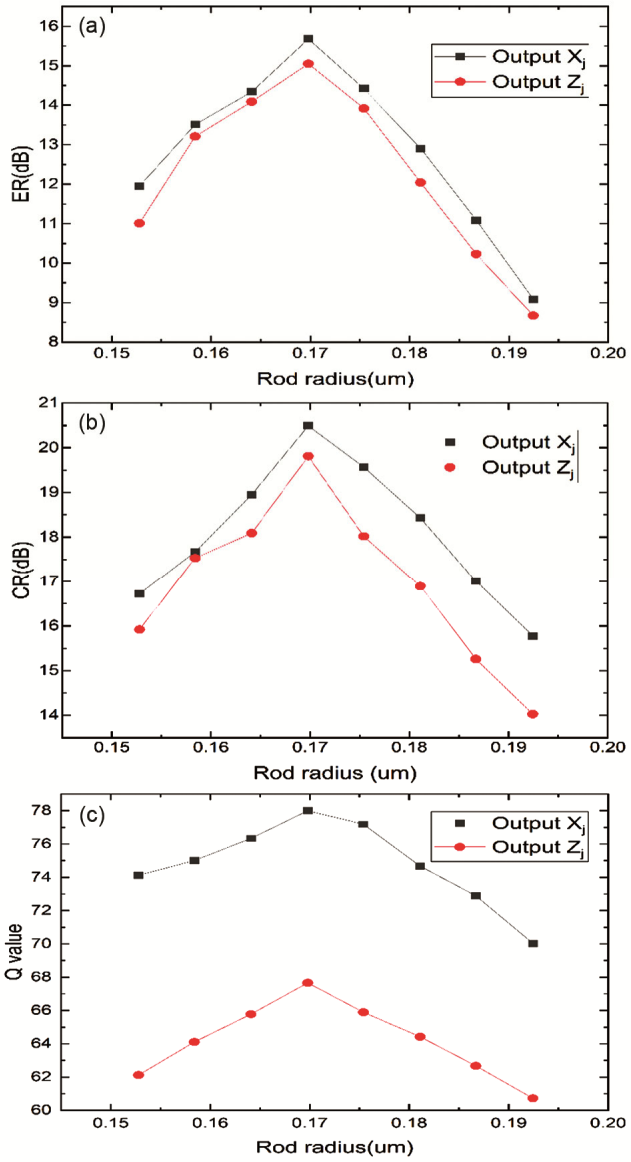


Fig. 11 — Variations of (a) ER (b) CR (c) Q value with rod radius of the N-bit comparator outputs Xj and Zj

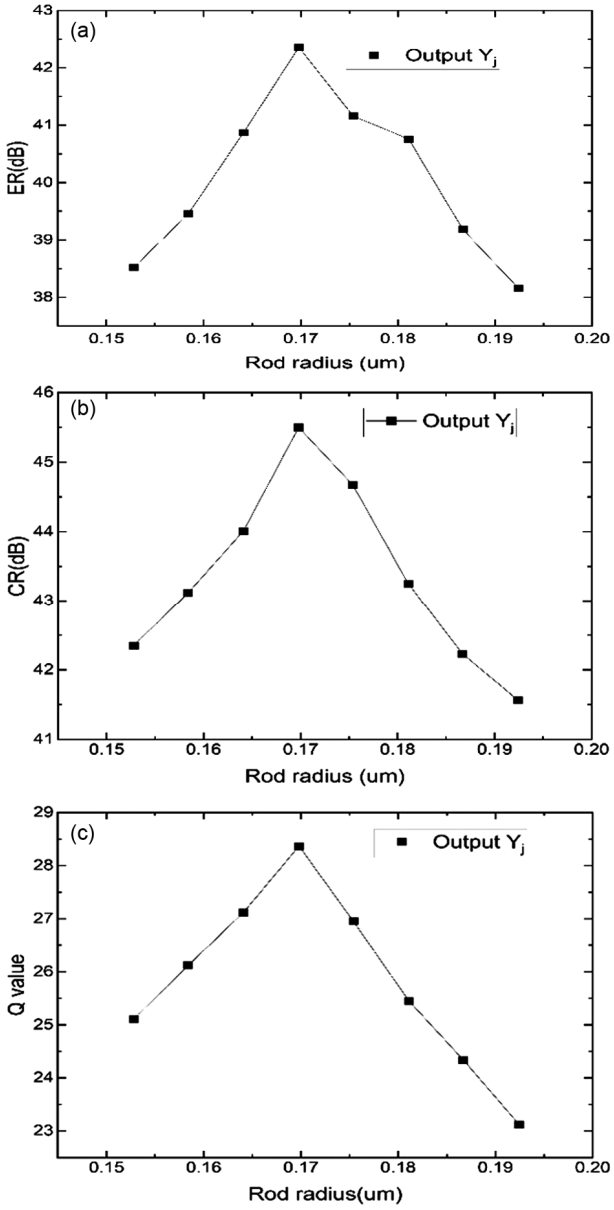


Fig. 12 — Variations of (a) ER (b) CR (c) Q value with rod radius of the N-bit comparator output Yj

Table 4 — optimized CR, ER, Q value of the comparator

| | Output port | | |
|---|---|---|---|
| | $X_j$ | $Y_j$ | $Z_j$ |
| CR(dB) | 20.49 | 45.5 | 19.814 |
| ER(dB) | 15.68 | 42.36 | 15.05 |
| Q | 78 | 28.37 | 67.66 |

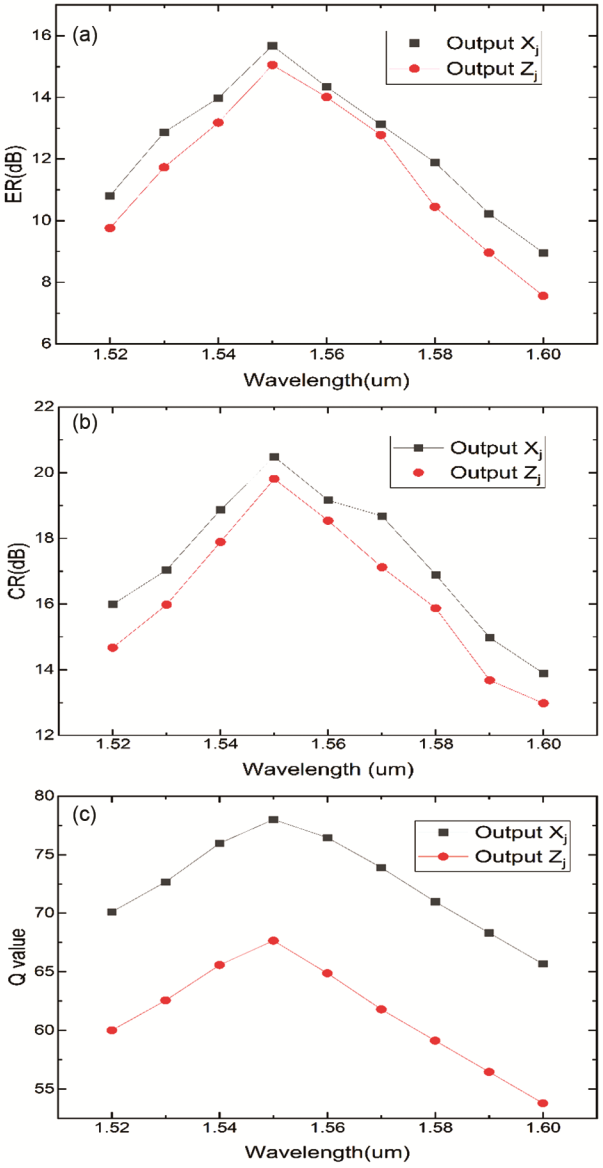


Fig. 13 — Variations of (a) ER (b) CR (c) Q value with wavelength of the N- comparator outputs Xj and Zj

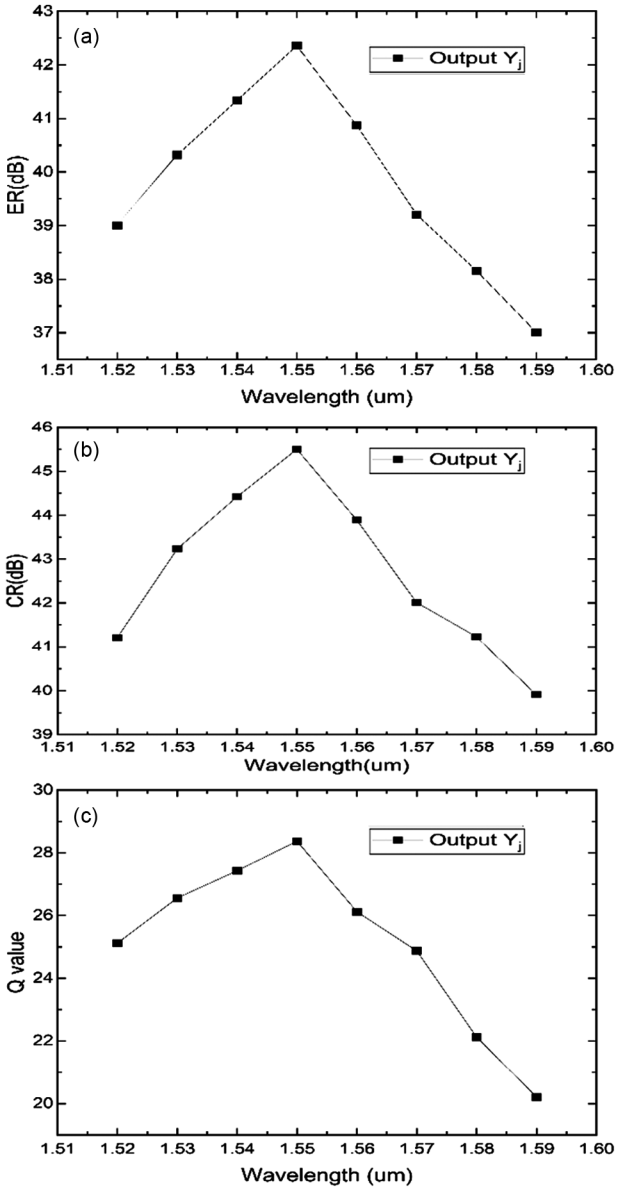


Fig. 14 — Variations of (a) ER (b) CR (c) Q value with wavelength of the N-bit comparator output Yj

## 4 Conclusion

The performance of the N-bit comparator is optimized by carefully selecting the refractive index and radius of the defect rods using 2D photonic crystals platform. An input signal wavelength of 1.55 µm is employed to ensure minimal transmission loss in silicon waveguides, aligning with the standard telecom band for practical compatibility. The values of ER, CR, and Q are 15.68 dB, 42.36 dB, 15.05 dB, 20.49 dB, 45.5 dB, 19.81 dB, 78, 28.37, 67.66. The high values of ER, CR, and Q indicating a highly efficient and reliable comparison mechanism. The device performs bit-wise serial comparison from the Most Significant Bit (MSB) to the Least Significant Bit (LSB), enabling ultrafast decision making with a data processing rate reaching up to 5 Tb/s. This ensures suitability for high-speed optical computing and signal processing applications.

## References

1 Arunkumar R & Robinson S, *Silicon*, 16 (2024) 4997.
2 Wei J, Yi Z, Yang L, Zhang L, Yang J Qin M & Cao S, *J Anal Methods,*16 (2024) 4901.
3 Jayanth C, Peter P S E & Santhosh B, *J Optics*, 53 (3) (2024) 2331.

4 Li H, Chen H, Li Y, Li S & Ma M, *Optics & Laser Technol*, 168 (2024) 109909.
5 LiuY, Neural Network Modelling of Point-Defect Microcavities in One-Dimensional Photonic Crystals, In *4th International Conference on Computer Science and Blockchain (CCSB)*, IEEE, p. 190-195 September 2024.
6 Rafiee E, *Plasmonics*, 19 (1) (2024) 439.
7 Gupta P K, Paltani P P & Tripathi S, *Physica Scripta*, 99 (11) (2024) 115541.
8 Elhachemi K & Rafah N, *J Opt Comm*, 44 (1) (2024) 283.
9 Kalra Y, Rani P & Sinha R K, Optical logic gates on photonic crystal platform, In *On-Chip Photonics,* Elsevier, 2024 p. 133-154.
10 De Almeida L C P, De Sousa F B, Junior W G P & Costa M B C, *J Comm Inform Syst*, 39 (1) (2024) 35.
11 Firouzimoghaddam A & Sharifi H, *J Comp Electron*, 24 (1) (2025) 1.
12 Bin A R, Rakshit J K, Kumar D, Yakkala B, Nagaraju V & Hossain M, *Appl Phys A*, 131 (1) (2025) 1.
13 Poursaleh A & Andalib A,*Optica Applicata*, 49 (3) (2019) 487.
14 Maji K, Mukherjee K & Mandal M K, *J Optics*, (2024)1.
15 Parandin F, *Optics & Laser Technol*, 144 (2021) 107399.
16 Moniem T A, El Deen E S & El Mayet R, *J Eng Sci*, 52 (4) (2024) 62.
17 Maji K, Mukherjee K & Mandal M K, *J Optics*, 54 (2024) 1518.
18 Michael M, Britto E C, Nizar, M & Anbarasan S D, *J Optics*, (2024) 1.
19 Moniem T A, *Opt Quant Electron*, 47 (2015) 2843.
20 Farid F, Vahideh & Andalib A, *Optik*, 172 (2018) 241.
21 Lian Z, Mehdizadeh F & Talebzadeh R, *Appl optics*, 58 (30) (2019) 8316.
22 Jile Hu Ge, *Appl Optics,* 59 (12) (2020) 3714.
23 Asghar A & Parandin F, *J Comp Electron* 22 (1) (2023) 288.
24 Fariborz P, Kamarian R & Jomour M, *Appl Optics*, 60 (8) (2021) 2275.
25 Zahra S, Soroosh M & Alaei-Sheini N, *Appl Optics*, 59 (3) (2020) 811.
26 Asghar A, *J Optic Comm*, 44 (1) (2024) 379.
27 Parimal G & Kumar Garai S, *Optik*, 122 (17) (2011) 1544.
28 Mirco S, *et al*, "Photonic processing for digital comparison and full addition based on semiconductor optical amplifiers." *IEEE Journal of Selected Topics in Quantum Electronics* 14 (3) (2008) 826-833.
29 Mukherjee, Kousik & Ghosh P, *Optik,* 123 (24) (2012) 2276.
30 30 Sukhoivanov I A & Guryev I V, *Photonic crystals: physics and practical modeling*, (Springer) 152, 2009.
31 Kiyotoshi Y, *Electromagnetic theory and applications for photonic crystals*, CRC press, 2018.
32 Yang H & Mittra R, *Artech house,* 2008.